A System for Rapid Design and Manufacturing of Custom-Tailored Shoes

Sangkun Park*
Institute of Advanced Machinery and Design, Seoul National University
Kunwoo Lee, Jongwon Kim, Jongwoo Park
School of Mechanical & Aerospace Engineering, Seoul National University

Rapid design and production techniques are indispensable for the custom-made production systems. For manufacturing custom-made shoes, the shoelast should be designed rapidly from the individual foot model. In this paper, we develop an integrated system for rapid design and manufacturing of custom-tailored shoes. The foot shape measurement sub-system allows scanning a standard shoelast and an individual foot and then extracts the three-dimensional cross-sectional data of the shoelast and the human foot shape from the captured image data. The shoelast design sub-system uses the scanned data to design new customized shoelast curves or surfaces with the heeling and mixing algorithms built in this system. The pattern design sub-system provides a method, which transforms a shoe-upper surface designed by a stylist into a flat-pattern that can be manufactured. We also export the surface model to an NC machine to manufacture the physical shoelast model.

Key Words : Custom-Tailored Shoes, Shoelast

1. Introduction

In recent years, production systems have moved away from mass production of a limited number of products to custom production in smaller volumes. In a typical custom production system, the customer orders the product on-line by providing product specification data. The product is then manufactured within a few days and delivered to the customer. In the particular case of shoe-production, the differences in foot shape and size, as well as individual stylistic preferences, make the application of a custom production system particularly appealing.

A careful examination of shoe market trends suggests that with advances in technology and lowering of costs, the demand for custom-tailored shoes will increase rapidly. A typical scenario in which custom-tailored shoes become readily available to the ordinary consumer can be envisioned as follows. The customer's foot is first scanned in a store, upon which the scanned foot data and the stylistic design chosen by the customer are then transferred to the manufacturing site through the Internet. At the manufacturing site, a suitable standard shoelast model [Miller, 1976] (a *shoelast*, or *last*, is a three-dimensional plastic or wood model of the foot that is used in the shoe manufacturing process) in the database is modified to satisfy the characteristic shape features of the foot model; the customized shoelast is then made from this modified last model. The shoes are then manufactured using the customized shoelast and immediately shipped to the customer.

The advantages of a custom tailoring footwear system are that the customer can select shoe styles to meet his or her tastes while satisfying the requirements of fit and comfort. From the manu-

* Corresponding Author,
E-mail : psk@cad.snu.ac.kr
TEL : +82-2-880-1685 ; **FAX** : +82-2-887-2283
Institute of Advanced Machinery and Design, Seoul National University, San 56-1, Shilim-Dong, Kwanak-Gu, Seoul, 151-742, Korea. (Manuscript **Received** December 21, 1999; **Revised** April 10, 2000)

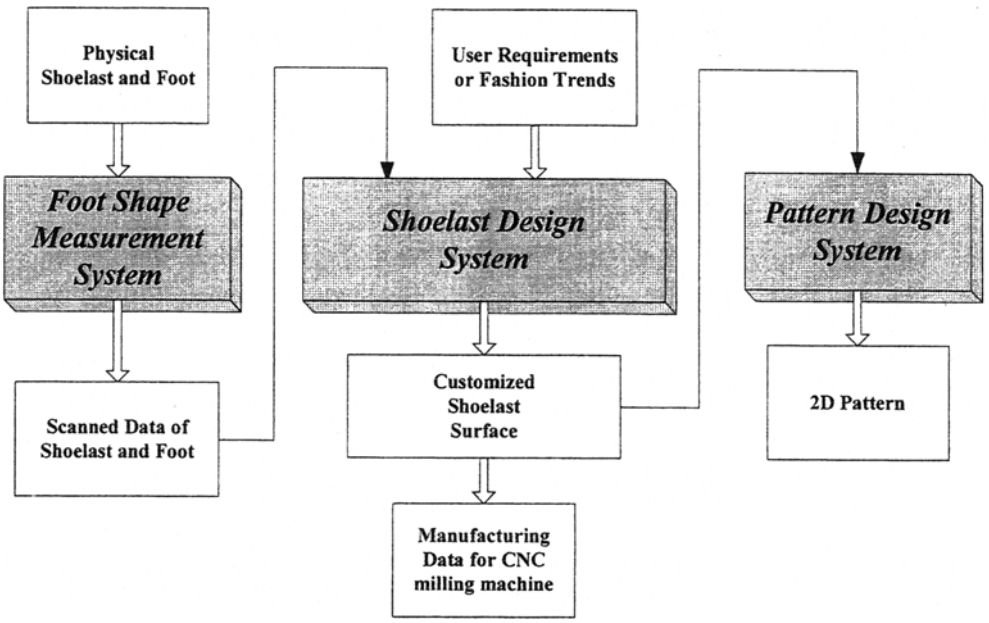

Fig. 1 Overview of configuration for custom-tailoring footwear system

facturer's perspective, a custom tailoring footwear system can mean smaller inventories, and the scanned foot data and other information on the customers can be stored for later use. If the foot data of enough customers is stored in the database, this information can also be used to develop standard shoelasts that can be applied in the mass production of ready-made shoes.

The components technology for a custom tailoring shoe system are now widely available, and we are witnessing a growing number of commercial systems based on the currently available technology. The *Shoemaster* System (http://www. shoemaster. co. uk/), developed by Clarks Ltd. in the U. K., is a system first introduced in 1965 that includes a module for 3D shoe CAD and manufacturing, a module for 2D shell grading, and a module for pattern assessment. The *Crispin* System (http://www. crispinsystems. com/), developed by the USM group Ltd in U. K., has similar features and functions as the Shoemaster; the main components are the Shoe-Design module for shoe design visualization and appraisal and last- and design-flattening, and the Pattern-Engineering module for 2D upper design, part-pattern development, and grading of the upper and bottom patterns. These systems have led the market for over ten years and are now focusing on expanding their capabilities to realize a custom tailoring footwear system.

There are many possibilities in the constitution of such a system, and important questions remain on how one can integrate the various components of such a system in a way that is economically viable without sacrificing performance. In this paper we describe our efforts in the development of a complete custom tailoring shoe system. The overall system shown in Fig. 1 consists of a foot shape measurement sub-system, a shoelast design sub-system, and a pattern design sub-system. The foot shape measurement system extracts the three-dimensional cross-sectional data of the human foot (or shoelast) from the captured image data. One of the crucial steps in this process is the calibration of the measurement system; we describe a novel algorithm for this purpose in Sec. 2. The shoelast design system in Sec. 3 uses the scanned data provided by the measurement system to design new shoelast curves or surfaces fitted to the scanned data. For the new shoelast geometry, we have developed a general geometric library for shoelast manipulation that provides heeling and mixing utilities as one of its capabilities. Finally, the patterning system for the shoe

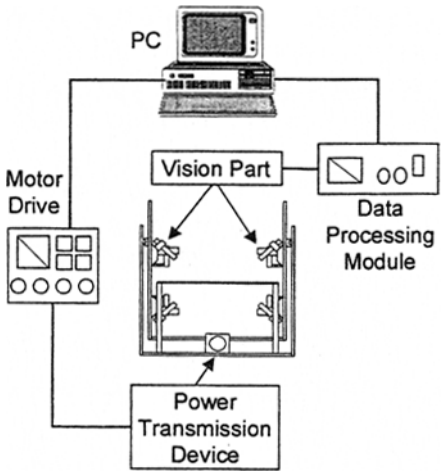

Fig. 2 Structure of foot shape measurement system

-upper transforms the shoe-upper (which can be regarded as a freeform surface) designed by a stylist into a flat-pattern that can be manufactured. The pattern system will be described in Sec. 4.

2. Foot Shape Measurement System

2.1 Structure of foot shape measurement system

Figure 2 shows the structure of the foot shape measurement system developed for the proposed system. The system consists of a power transmission part, a vision part and a control part. The power transmission part is composed of a torque motor, a motor control drive and a lead screw mechanism. The vision part is composed of a slit beam laser, a CCD camera and a moving plate. The control unit controls the motion, scanning and storing of the measurement data.

2.2 Measurement of the foot sole

A sole measuring unit has two main functions. One is to apply pressure to a sole appropriately and the other is to scan the shape of the sole at that state. The three-dimensional shape of a sole is measured in the distorted state by an appropriate pressure, because soles are typically pressured under walking conditions. The first step in the development of a sole measuring unit is to determine the applied pressure condition, and the next

Fig. 3 Foot-print on a form-art

is to design an appropriate mechanism for applying the desired pressure field to a sole.

Three different types of units are suggested. The first is to measure the footprint on form-art, a sponge-like material. The second is to extract the shape of the sole from the position difference data obtained from an array of movable pins. The third is to scan the foot shape on transparent glass using the slit beam laser projection technique.

For our system the slit beam laser projection technique is used to scan a sole under distortion. A scanning part that consists of the laser slit beam and a CCD camera is fixed to a moving plate. The moving plate then repeats a moving and scanning procedure over a fixed interval.

Type 1. Using the foot-print on form-art

Form-art is a material that plastically deforms under physical pressure. A typical foot-print on form-art is shown in Fig. 3. The sole shape impressed into the form-art is then scanned using the slit beam laser projection technique. There are a number of drawbacks associated with this method. From a material perspective, form-art is expensive and not reusable, and the available colors and hardness are limited (the color of form-art affects scanning performance). From a measurement perspective, the scanning of the sole and instep are performed separately, meaning the scanning process must be repeated. This results in a lengthy total process time, clearly a disadvantage from a rapid manufacturing viewpoint.

Type 2. Using a spring-supported pin array

An array of pins, with each pin supported by a spring, will undergo a series of linear displacements when the client stands on this pin array.

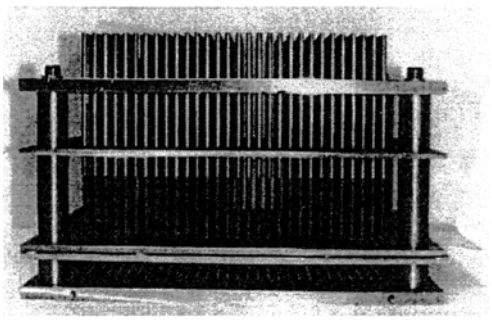

Fig. 4 Spring-supported pin array

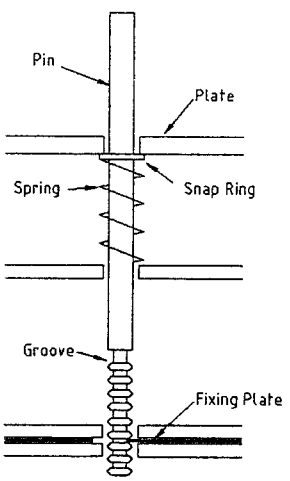

Fig. 5 Schematics of a pin fixing part

This position data can be measured to obtain the sole shape data.

The unit is composed of the body plate, the pins and springs, and a fixing plate as shown in Fig. 4. When the foot is placed on the upper plate, each pin is changed in position due to body weight and the spring force. At the lower part of the pin, there are 17 grooves inclined at plus and minus 45 degrees successively, and each pin is fixed by inserting a fixing plate to a groove as shown in Fig. 5. Each fixing plate has the same number of holes as the number of pins, so it fixes all of the pins at the same time. After removing the foot off the plate, the crown of a pin is scanned using the slit beam laser projection technique. After this the fixing plate is set to an initial state by pushing to the original position and the entire pin is reset to the initial position by the spring force. The scanned data is then used to extract the distorted shape of the sole.

The disadvantage of this unit is that the fixing plate does not fix all the displaced pins. Only 40 pins among the entire 400 pins are fixed in our test and the remaining pins are reset to the initial position by the spring reaction force. This is because some holes are in contact with the peak of a groove, the other holes can no longer be in contact with the valley of the groove.

Even if all pins are fixed with the fixing plate, there is a problem in a data distribution. The distance between pins is fixed at 10 mm in this unit, so the data resolution is fixed. As a result, there is a limit error in interpolation. Furthermore, the distance between pins has a limit in the physical model.

In the measuring process, scanning the crown of the pin and the foot instep are separated, so the scanning process must be repeated. Fixing a pin is done manually, requiring intervention on the part of the user. From a rapid manufacturing perspective, these features are undesirable that only serve to lengthen total process time.

Type 3. Using a transparent glass

In this method, after the customer steps onto the glass, the sole on the glass is scanned by a vision module consisting of two pairs of a slit beam laser and a CCD camera under the glass. By setting an additional scanning part consisting of two pairs of the silt beam of a laser and a CCD camera over the glass, an instep of the foot can be scanned simultaneously. Therefore the measurement hardware and associated measuring technique can be simplified and the total scanning time shortened. Figure 6 shows the physical hardware configuration.

The hardware configuration consists of three parts as shown in Fig. 7 — a frame composed by plates, a vision part composed by the silt beam of a laser and a CCD camera, and a power transmission part composed by a step motor, a motor drive and a lead screw. A rotational movement of a motor is transferred to a linear motion of a screw-nut using a lead screw. A moving part connecting to a screw-nut can move forward or backward linearly in the horizontal direction. There is a vertical direction slot in the side plate,

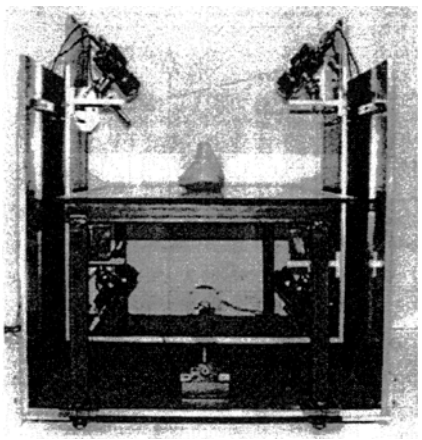

Fig. 6 Measurement configuration using transparent glass

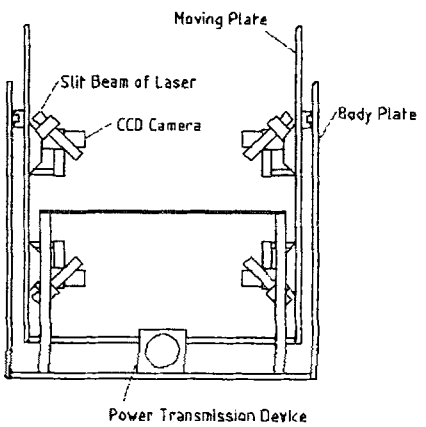

Fig. 7 Scanning modules

which attaches the slit beam laser and a CCD camera. Therefore the position of the slit beam laser and the CCD camera can be regulated in the vertical direction.

In the 300 mm range, the vision module scans the foot shape by repeatly moving and scanning at fixed intervals of 4 mm . The laser scanner and a CCD camera placed at the four corners measures the foot shape in order. With this unit it takes approximately 108 seconds to measure the foot shape.

The measurement time is an important performance index of this unit with respect to rapid manufacturing. Three ways are suggested to reduce the measurement time of this unit. The first one is to reduce the weight of a moving plate. The second one is to re-design the power transmission module. The last method is to improve the control algorithm of motor.

2.3 Measurement of an instep of the foot

An instep of the foot is measured in unloading condition. Nowadays a coordinate measurement machine (CMM) is used to measure a three-dimensional shape in engineering area. CMM measures coordinate values of points on a object using a contact probe. But it takes a long time in the application that needs many data point. For this reason, non-contacting methods including optical triangulation and stereo-vision are widely studied. Among them, a three-dimensional free surface measurement technique using the slit beam of a laser projection shows a 0.1-0.2 mm measuring resolution in a rapid 3 dimensional measurement using a computer vision technique. A measurement unit of an instep of the foot is designed based on the slit beam of a laser projection technique. The following things are considered in constructing a measurement unit of an instep of the foot. At first the slit beam of a laser and a CCD camera should be appropriately arranged to entirely measure a free surface of a instep of the foot — a wrinkle, a heel and a top and two sides of the foot. Secondly a data processing device obtaining a shape data of the foot is constructed so that a CCD image data is digitized to a point cloud data containing a foot shape.

2.4 Calibration

Camera calibration in 3D computer vision is the process of determining the intrinsic and extrinsic calibration parameters. The intrinsic parameters are the optical characteristics of camera, such as focal length, optical center, and radial distortion coefficient. The extrinsic parameters are the relation between the world coordinate system and the computer image coordinate system.

There have been many researches on calibration. Recently, the self-calibration technique is widely used because of its convenience and efficiency. Tsai proposed a self-calibration technique that can be applied to general calibration process in 1987. In the proposed system, Tsai's technique

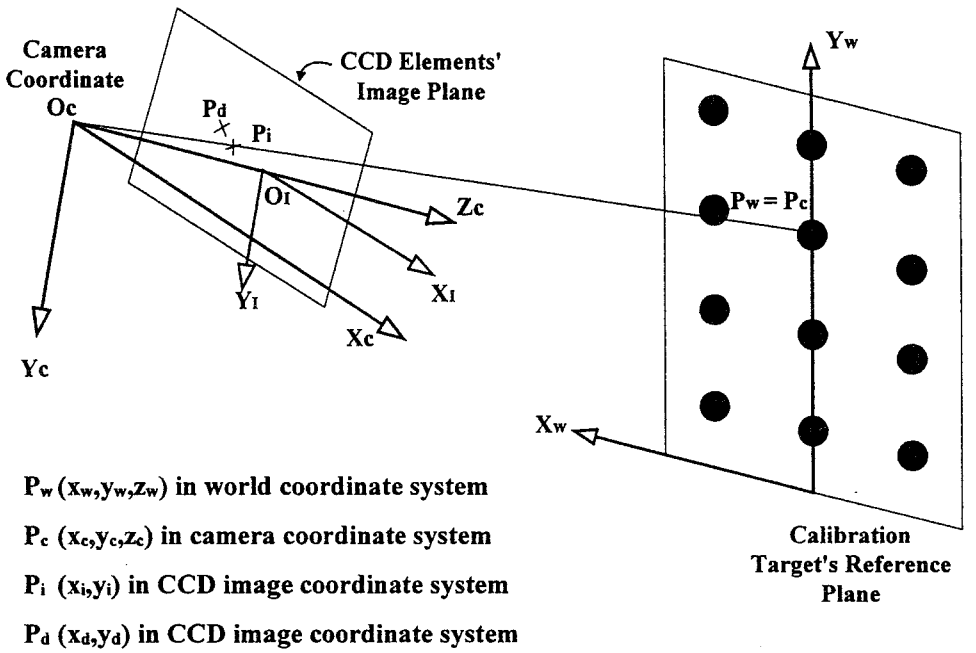

Fig. 8 Calibration Geometry

is used with some modification.

2.4.1 Calibration principle

A pin hole camera model and the corresponding perspective projection are used as shown in Fig. 8. There are circles on the face of calibration target which exists in the world x-y plane. The center points of the circles are used as calibration points denoted by $P_w(x_w, y_w, z_w)$ in world coordinate system and $P_c(x_c, y_c, z_c)$ in camera coordinate system.

P_c should be projected onto $P_i(x_i, y_i)$ on the CCD image plane by a perspective transformation. However, in real situation, P_c is projected to $P_d(x_d, y_d)$ on the CCD image plane due to lens distortion effect. The point P_d appears on the computer screen image via the frame grabber and we denote the displayed point by $P_f(x_f, y_f)$ defined in the computer image coordinate.

Using the mapping between the coordinate of a calibration point in the world coordinate system and the coordinate of the calibration point in the computer image coordinate system, we can define the calibration parameters as follows:

Relation 1: Relation between the world coordinates and the camera coordinates

$$\begin{bmatrix} x_c \\ y_c \\ z_c \end{bmatrix} = \begin{bmatrix} & & & P_x \\ \alpha & \beta & \gamma & P_y \\ & & & P_z \end{bmatrix}^{-1} \cdot \begin{bmatrix} x_w \\ y_w \\ z_w \end{bmatrix} \tag{1}$$

where α, β, γ=Z-Y-X Euler angles (Craig 1986) and

(P_x, P_y, P_z) =translation vector

Relation 2: Relation between the camera coordinates and the ideal image coordinates

$$x_i = f\frac{x_c}{z_c} \tag{2}$$

$$y_i = f\frac{y_c}{z_c} \tag{3}$$

where f=effective focal length.

Relation 3: Relation between the ideal image coordinates and the real image coordinates in the CCD image coordinate system

$$x_d = (1+\kappa_c r^2)^{-1} x_i \tag{4}$$

$$y_d = (1+\kappa_c r^2)^{-1} y_i \tag{5}$$

where $r=\sqrt{x_d^2+y_d^2}$ and κ_c=radial distortion coefficient.

Relation 4 : Relation between the real image coordinates in the CCD image coordinate system and the computer image coordinates

$$x = s_x d_x x_d + C_x \quad (6)$$

$$y = s_y d_y y_d + C_y \quad (7)$$

Where d_x, d_y=relation between the real image units in CCD image coordinate system and the pixel units in the computer image coordinate system

C_x, C_y=optical center of the camera, and

s_x, s_y=uncertainty coefficients due to frame grabber's operation

Note that s_x was not used in Tsai's coplanar calibration technique although he introduced the term. In this paper, we considered both terms and computed through an additional optimization process.

2.4.2 Calibration procedure

The calibration procedure has been implemented in the proposed system as follows:

a. The world coordinates of all calibration points are specified and their corresponding computer image coordinates are obtained by image processing.

b. The image processing includes the threshold operation to define the circle region on the image and the average calculation to find center of the circle in the computer image coordinates.

c. Calibration parameters except s_x, s_y are approximately calculated by applying Tsai's coplanar calibration algorithm.

d. Using the approximated parameters as an initial value, all the calibration parameters are computed by the following optimization scheme.

Find all calibration parameters such that $\frac{1}{2}\sum_{i}^{n}|P_{w,i} - P_{wc,i}|^2$ is minimized.

where $P_{w,i}$ means real world coordinates of the i-th calibration point and $P_{wc,i}$ indicates the calculated world coordinates corresponding to the $P_{w,i}$ by using the calibration parameters. n is the number of calibration testing points. Note that we can obtain more accurate results when n is increased.

2.5 Scanning

To scan the whole shape of shoelast or foot, we use four cameras and four slit beam lasers. In a certain position, the lasers project the slit beam on the shoelast or foot surface, so the reflected slit beam makes a contour shape on the plane that is parallel with x-y plane in world coordinate system. At this moment, the cameras take the picture of the shoelast or foot. Each camera covers the partial region of shoelast or foot; left upper, right upper, left lower, and right lower parts as shown in Fig. 9.

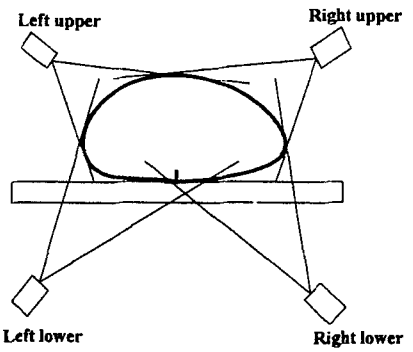

Fig. 9 Camera coverage area

Both the captured image data and the corresponding laser location are stored in the buffer for later calculation. Both cameras and lasers move to the next position and the same process as described above is repeated. The moving direction coincides with z-axis of the world coordinate system, and the moving interval distance is determined by user's specification.

From the calibration process explained in the previous section, it is known that one point defined in computer image coordinates exists anywhere in the line that passes both the camera center and the corresponding point on the reference plane. However, the 3D position of a computer image point can be computed by using the calibration parameters and laser location data as follows:

For a point in computer image coordinate, the corresponding ideally projected point, P_1 in the CCD image coordinate is calculated from Eqs. (4) through (7).

Substituting $P_1(x_1, y_1)$ into Eq. (2) and (3), we obtain

$$x_c = C_1 z_c \qquad y_c = C_2 z_c \quad (8)$$

where $C_1 = \frac{x_i}{f}$, $C_2 = \frac{y_i}{f}$

And substituting Eq. (8) to Eq. (1), we obtain

$$\begin{aligned} x_w &= (\cos\alpha\cos\beta)\, C_1 z_c + (\cos\alpha\sin\beta\sin\gamma \\ &\quad -\sin\alpha\cos\gamma)\, C_2 z_c + (\cos\alpha\sin\beta\cos\gamma \\ &\quad +\sin\alpha\sin\gamma)\, z_c + P_x \\ y_w &= (\sin\alpha\cos\beta)\, C_1 z_c + (\sin\alpha\sin\beta\sin\gamma \\ &\quad +\cos\alpha\cos\gamma)\, C_2 z_c + (\sin\alpha\sin\beta\cos\gamma \\ &\quad -\cos\alpha\sin\gamma)\, z_c + P_y \\ z_w &= (-\sin\beta)\, C_1 z_c + (\cos\beta\sin\gamma)\, C_2 z_c \\ &\quad + (\cos\beta\cos\gamma)\, C_2 z_c + P_z \end{aligned} \tag{10}$$

As P_w is located on the laser-reflected curve, z_w is known from the laser location. Thus, z_c is calculated as follows:

$$z_c = \frac{z_w - P_z}{-C_1\sin\beta + C_2\cos\beta\sin\gamma + \cos\beta\cos\gamma} \tag{11}$$

Substituting Eq. (11) into Eq. (10), x_w and y_w position of the point are derived.

3. Shoelast Design

3.1 Custom-tailored shoelast design

In shoe manufacturing, shoelasts are essential because they dictate the exact shape, size, and fit of the shoes made on them. Shoelast design depends on fashion trends as well as on the anatomy of the foot.

Except a few cases which involve soft upper materials and where shape is not important, all footwear is made on a shoelast. A shoelast is a foot-shaped block of hard and stable material that gives footwear its shape. Although foot -shaped, a shoelast is not an exact copy of a foot. Its shape is dictated by some factors such as fit and comfort, ease of manufacture, and fashion. The factors could be simply neither measured nor formulated with scientific knowledge. So, the current technology for shoelast design depends on the experimental data and its statistical analysis or the experience of some specialists or engineers.

Figure 10 shows the traditional process of the shoelast design [Miller, 1976]. First the designer studies on the anatomy of a foot, and measures the size of the foot in accordance with the anatomy. Based on the measurements, the shoelast is designed and the shoes are made on the obtained shoelast. Now the tester wears the shoes and

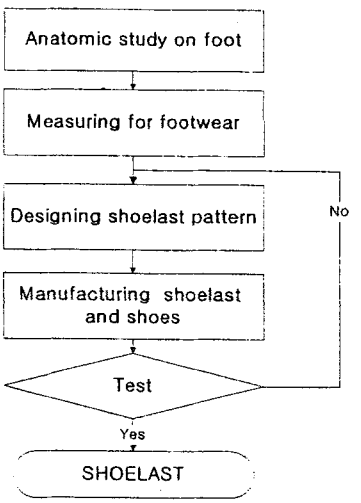

Fig. 10 Traditional process of shoelast design

reports the defects of the shoes. According to the report, the shoelast is modified until the test result is satisfactory.

This traditional shoelast design process is inefficient because one should repeatedly make many prototypes of shoelast and footwear to test fitness and comfort. Cho studied on the relation between a foot and a shoelast. He first studied foot anatomy, and the function and structure of a foot. From these he determined the main measuring points. He built up the database of the relations according to age, gender, and regional groups. He also gathered the test results to construct the database. Then the dimension and the size of shoelast at the main measuring points are determined by a statistical method. He recommended the representative data or table by determining the standard values based on the foot length and girth.

The traditional design process as well as Cho' s method plays an important role in realizing the custom-tailored shoelast design system. However, they do not provide the core technology for building a strict custom-tailored system. The reason comes from that the custom-tailored system requires shoelast fitting each individual rather than the standard shoelast having more or less larger deviations in statistical analysis. Thus it is necessary to modify the detailed shape of the existing standard shoelast model considering the

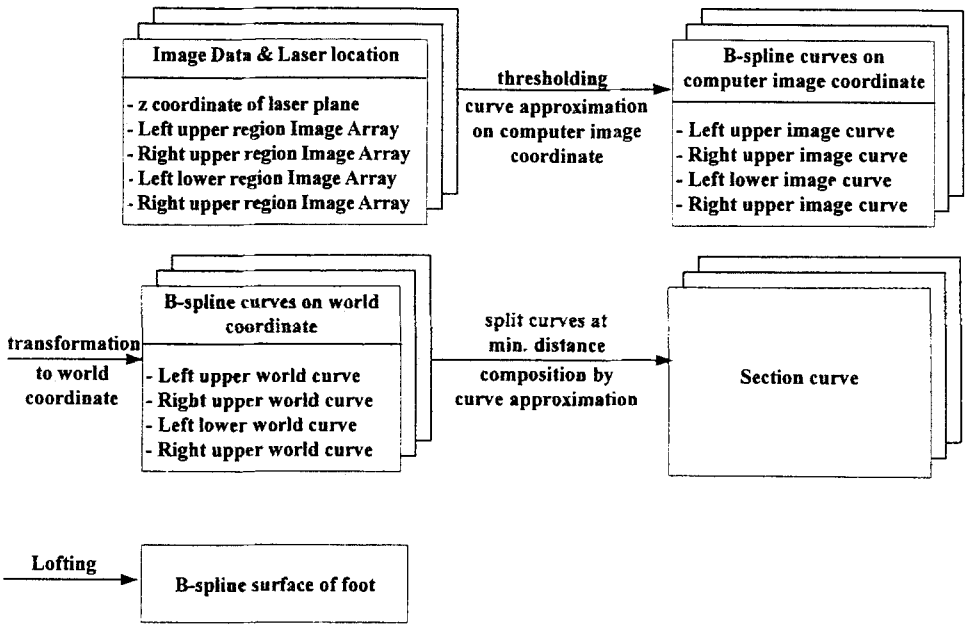

Fig. 11 A procedure for making a foot surface

individual foot shape in views of factors such as fit, comfort, ease of manufacture, and fashion.

3.2 Making a foot surface

From the image data stored in section 2.4, the computer image coordinates of the reflected slit beam in pixels are obtained by threshold operation. From the pixel clouds, a B-spline curve in the computer image coordinate system is derived. [Piegl, 1995] Because the thickness of slit beam is much bigger than the thickness of one pixel, the least square curve approximation technique is used to find a curve that passes the center of the point clouds. Then by transforming the control points of the curve as described in section 2.4, a B-spline curve of the laser reflected contour is obtained in world coordinate system.

Four world curves can be derived from the image data of each partial region. Then the four world curves are merged into a single closed curve. Here, the four curves are generally overlapped at their connection region. So a composite procedure dealing with the overlapped region is proposed. That is:

a. For two curves to be connected, find the location on each curve at which the distance between two curves is minimal.

b. Split each curve at the corresponding location found in step (a).

c. Delete the fully overlapped curve of two split curves.

c. Sample the points on the remainder of each split curve.

d. From the sampled points, obtain a composite curve by approximation.

To obtain the whole section curves, the above process is repeated for each section curve. Then a lofted B-spline surface is obtained from the section curves. The whole process is shown in Fig. 11.

3.3 Heeling

In foot shape measurement system, both a shoelast and a foot are measured without a heel elevation. In this section, we describe a heeling algorithm that enables two measured data to have the same heel elevation or height. Note that the same elevation is necessary for mixing the two objects. The mixing algorithm will be explained in the next section.

The heeling algorithm is explained in Fig. 12. The heeling process for shoelast requires a simple

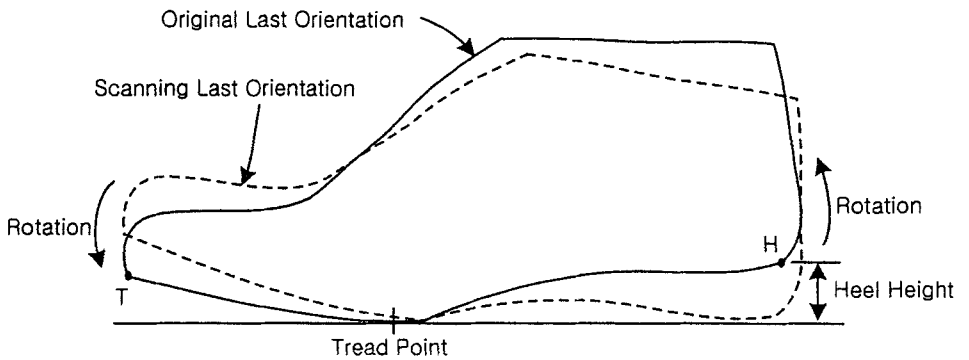

(a) Shoelast heeling

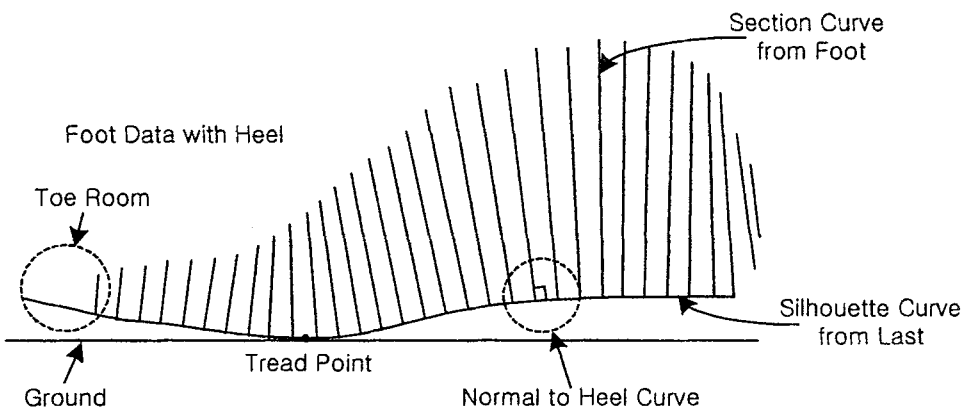

(b) Foot heeling

Fig. 12 Heeling of shoelast and foot

rotation of measured last at the tread point shown in Fig. 12 (a), while the foot heeling process demands a complex transformation by the silhouette curve derived from the shoelast shown in Fig. 12 (b).

Both the heeling processes are described as follows:

a. The last is rotated by the heel height using the tread point as a center of rotation, which is shown in Fig. 12 (a).

b. A silhouette curve of the last sole is obtained from point T to point H after the rotation. See Fig. 12 (a). The silhouette curve is generated with the closest point of each last section curve to the ground. These closest points are interpolated to obtain a B-spline curve.

c. A foot is moved so that the tread point is coincident with the last. See Fig. 12 (b). Since it is not easy to find the tread point from human foot, a head point of metatarsal bone from X-ray is projected onto the ground. This is taken as a tread point.

d. The orientation of each foot section curve is determined by the silhouette curve so that the angles between the silhouette curve and each section curve are orthogonal to each other. See Fig. 12 (b). The interval distance between foot section curves is uniformly scaled and distributed along the silhouette curve.

3.4 Mixing

The mixing functionality is one of the most important factors in our custom-tailored shoelast design system. It blends the features of the scanned standard last and the human foot shape. The blended shape is close to the human's one so that he/she feels comfortable. In addition, the proposed system lets the designers add new fash-

(a) Shoelast

(b) Foot

(c) Mixed curves

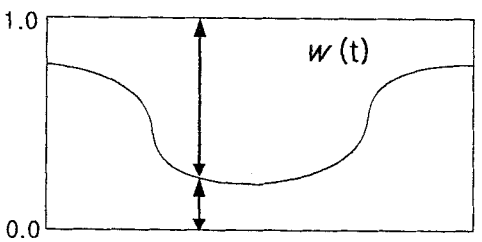

(d) Weighted distribution curve

Fig. 13 A mixing example with predefined weighted distribution curve

ion into the blended output. The current technology of the shoelast design makes focus on fashion rather than human factors aspect. It results in uncomfortable footwear. There have been many researches related to the anatomy and biomechanics regarding the problems of feet. But most of outstanding studies depend on their clinical experiments and not based on theoretical formulation.

In this work, a weighted distribution function is proposed to reflect the comfort. Although the comfort could not be measured or formulated with scientific knowledge in the current technology, it is possible to represent the comfort by the weighted function and to provide the modeling technique for a shape deformation.

Given the weighted distribution function, the mixing process in the proposed system is described as follows:

a. The heeled last and foot section curves are used to make the last and foot surfaces, respectively. Here, the B-spline surface is used.

b. The new intersection curves are generated from both the last and the foot surfaces with the equally and parallel spaced planes. See Fig. 13 (a) and (b).

c. A weighted distribution function predefined in our system or designed by user is used to blend two section curves: one from shoelast and the other from foot. Note that two section curves have the same z coordinate in the world coordinate system. See Fig. 13 (c) for the mixed section curves and (d) for the weighted distribution curve used in Fig. 13 (c). The mixed B-spline curve is computed as follows:

$$C_{mixed}(t) = w(t)\,C_{Lost}(t) + (1 - w(t))\,C_{Foot}(t)$$

where $C_{Last}(t)$ = Section curve of shoelast
$C_{Foot}(t)$ = Section curve of foot

(a) Shoelast surface (b) Foot surface (c) Mixed surface

Fig. 14 Comparison of shoelast, foot, and mixed surface

$C_{mixed}(t)$ = Mixed section curve

$w(t)$ = Weighted distribution curve

d. The mixed section curves are used to construct a surface by lofting method. The lofted surface reflects the weighted shape between shoelast and foot. See Fig. 14 (a), (b) and (c) for the shoelast, the foot and the weighted surface, respectively. Note that our system enables users to edit the weighted distribution curves for the improvement of foot comfort, new fashion, and others.

4. Pattern Design for Shoe-Upper

Following the shoe-last design system, the patterning system for the shoe-upper is developed. The shoe-upper can be considered as the set of freeform surfaces composed of several leather pieces. Traditionally a stylist designs the shoe-upper on the shoe-last and then a pattern-maker develops the shoe-upper surface into the 2D plane for pattern manufacturing. But generally the freeform surface in three dimensional Euclidean space is not developable because the Gaussian curvature of the points in the surface is not zero. So in most cases the process of flat-patterning is generally left to the manufacturer who generates the flat-pattern using heuristic methods. Our objective is to provide a method which can be implemented in an automated method for doing flat-patterning of shoe-upper surfaces.

The flat-patterning in shoe-making can be considered as the case of the developable surface

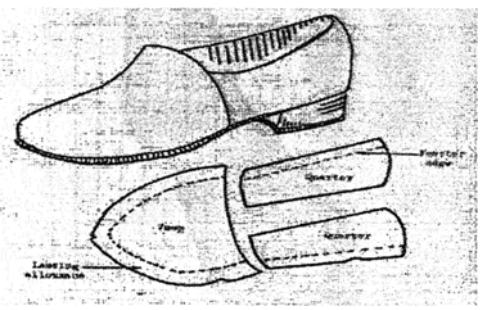

Fig. 15 A basic shoe-upper

design. Certain fabric and leather objects are made using patterns made from planar sheets. Since developable surfaces can be unrolled onto a plane without distortion, they can be cut from planar sheets, bent back into their final position, and stitched together. So we can obtain the proper flat-pattern for the given shoe-upper surface through approximating the surface by the proper developable surface. Figure 15 shows a basic shoe-upper.

In many practical situations one will find freeform surfaces manually approximated and assembled as sets of piecewise developable surfaces. We handle the developable surface approximation problem by dividing it into several procedures. We first approximate the shoe-upper whose boundary consists of freeform surfaces by the ruled surface. And in next stage we approximate the ruled by the developable.

Elber proposes a two-stage scheme to this surface approximation problem, in which the freeform surface is first approximated by a ruled

surface, and then the ruled surface approximated by a developable. Because ruled surfaces are much less restrictive than developable surfaces, the first stage approximation can be accomplished quite easily. We follow the Elber's approach in the first ruled surface approximation stage. When the B-spline surface is given, the ruled surface is obtained by projecting the control points along the ruled direction into the line connecting each control point for both isoparametric base curves. And in the second stage the ruled surface approximtion by the developable surface, as we now show, is accomplished quite naturally within our developable surface design algorithm.

4.1 Optimal control and the design of developable surfaces

In this section we formulate the developable surface design problem in an optimal control setting [Park, 1999]. Given a regular curve $\mathbf{b}(t)$ on the unit sphere corresponding to a one-parameter family of rulings, and two base curve endpoints $\mathbf{a}_0$, $\mathbf{a}_1 \in \mathbf{R}^3$, we consider the problem of constructing a base curve $\mathbf{a}(t)$ such that $\mathbf{a}(t_0) = \mathbf{a}_0$, $\mathbf{a}(t_1) = \mathbf{a}_1$, and the resulting surface $\mathbf{f}(s, t) = \mathbf{a}(t) + s \cdot \mathbf{b}(t)$ is developable. We formulate the base curve design problem as an optimal control problem, and derive solutions for objective functions that reflect practical aspects of developable surface design, or approximating a given arbitrary ruled surface by a developable surface.

We begin by recalling some basic facts about developable surfaces. Let be a regular curve in $\mathbf{R}^3$, and $\mathbf{b}(t)$ a differentiable curve in $\mathbf{R}^3$ such that $\|\mathbf{b}(t)\| = 1$ for all t ; here $\|\cdot\|$ denotes the standard Euclidean norm. Both curves are defined over some interval $[t_0, t_1]$. The parametrized surface

$$\mathbf{f}(s, t) = \mathbf{a}(t) + s \cdot \mathbf{b}(t),\ t \in [t_0, t_1],\ s \in \mathbf{R}$$

is called a ruled surface; $\mathbf{a}(t)$ is called the base curve, and the line passing through $\mathbf{a}(t)$ that is parallel to $\mathbf{b}(t)$ is called the ruling of the surface $\mathbf{f}$ at $\mathbf{a}(t)$. The ruled surface $\mathbf{f}$ is said to be developable if

$$\langle \mathbf{a}_t, \mathbf{b} \times \mathbf{b}_t \rangle = 0$$

where $\langle \cdot, \cdot \rangle$ denotes the Euclidean inner product in $\mathbf{R}^3$. This condition implies that the vectors $\mathbf{a}_t$, $\mathbf{b}$ and $\mathbf{b}_t$ are always coplanar. The condition for $\mathbf{f}(s, t)$ to be developable, namely, $\langle \dot{\mathbf{a}}, \mathbf{b} \times \dot{\mathbf{b}} \rangle = 0$, is therefore equivalent to the statement that $\dot{\mathbf{a}}$ must always lie in the plane spanned by $\mathbf{b}$ and $\dot{\mathbf{b}}$. That is, $\dot{\mathbf{a}}(t) = \mathbf{b}(t)\mathbf{u}_1(t) + \dot{\mathbf{b}}(t)\mathbf{u}_2(t)$ for some scalar functions $\mathbf{u}_1(t)$ and $\mathbf{u}_2(t)$.

By recasting the base curve design problem in the above form, we can appeal to the following well-known result on the controllability of linear time-varying systems to answer the question of existence of a solution. We can show that as long as the ruling $\mathbf{b}(t)$ is not a geodesic, the solution exists.

4.2 Optimal surface approximation and development

In this section we illustrate the optimal control approach to optimal surface approximation. By constructing an objective function whose solution finds the best developable surface approximation to a given ruled surface we can accomplish a crucial step to flat patterning.

Let the ruled surface be given by $\mathbf{r}(s, t) = \mathbf{c}(t) + s \cdot \mathbf{b}(t)$ where $\mathbf{c}(t)$ is the base curve and $\mathbf{b}(t)$ is the ruling, $t_0 \le t \le t_1$, $0 \le s \le L$. The objective then is to determine the base curve $\mathbf{a}(t)$ for the developable surface $\mathbf{f}(s, t) = \mathbf{a}(t) + s \cdot \mathbf{b}(t)$ that minimize

$$\frac{1}{2}\int_{t_0}^{t_1}\int_{0}^{L} \|\mathbf{f}(s, t) - \mathbf{r}(s, t)\|^2 ds\, dt$$

subject to $\dot{\mathbf{a}}(t) = \mathbf{B}(t)\mathbf{u}(t)$, with end point conditions $\mathbf{a}(t_0) = \mathbf{a}_0$ and $\mathbf{a}(t_1) = \mathbf{a}_1$. The above formulation ensures that the rulings of the developable surface coincide with those of the ruled surface at the base curve end points $t = t_0$ and $t = t_1$.

By a straightforward calculation, the above objective function reduces to

$$\frac{1}{2}\int_{t_0}^{t_1} \|\mathbf{a}(t) - \mathbf{c}(t)\|^2 dt$$

But the above choice of objective function leads to singular arcs; because $\mathbf{H}_{uu} = 0$, the optimal control will typically contain discontinuities, resulting in a discontinuous surface. To circumvent the singular arc problem, we propose instead

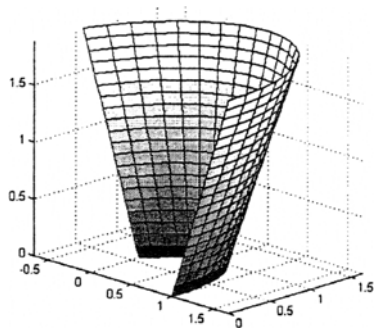

(a) A ruled surface

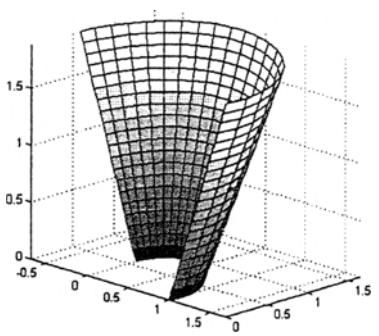

(b) Approximated developable surface

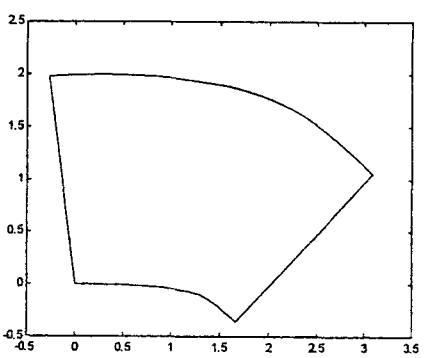

(c) 2D pattern of the developable surface

Fig. 16 Simulation results for pattern design

the following objective function:

$$\frac{1}{2}\int_{t_0}^{t_1}\int_0^L \alpha\|\mathbf{f}(s,t)-\mathbf{r}(s,t)\|^2+\beta(\|\mathbf{f}_t(s,t)-\mathbf{r}_t(s,t)\|^2+\|\mathbf{f}_s(s,t)-\mathbf{r}_s(s,t)\|^2)\,ds\,dt$$

subject to the same dynamic equation and boundary conditions. It can be readily shown that this objective function reduces to

$$\frac{1}{2}\int_{t_0}^{t_1}\alpha\|\mathbf{a}(t)-\mathbf{c}(t)\|^2+\beta\|\dot{\mathbf{a}}(t)-\dot{\mathbf{c}}(t)\|^2 dt$$

where α and β are arbitrary constant weighting factors. The optimal base curve $\mathbf{a}(t)$ can be obtained by solving a linear two-point boundary value problem.

Through the above procedures we can accomplish the design of the developable surface and then it can be developed into plane - because between the developable and the plane an isometric mapping exits. This process is a pattern development. Using the fact that curves on isometric surfaces have the same geodesic curvatures we can obtain the flat-pattern without much difficulties. We integrate the Frenet-Serret formula for the planar curve $\dot{\mathbf{t}}=\kappa_g\mathbf{n}$ where κ_g is the geodesic curvature of the corresponding curve on the developable surface.

Figure 16 (a) through (c) show simulation results for the optimal developable approximation to the ruled surface.

5. Conclusion

In this paper, we have proposed a complete system for rapid design and manufacturing of custom-tailored shoes. By scanning a standard shoelast and a human foot, we generate the B -spline section curves with the calibration and the scanning algorithms proposed in the paper. We then construct the new customized shoelast surface with the help of heeling and mixing functions. With this designed surface, we make a flat -pattern by the automated construction of a ruled surface and its developable surface approximation. We also export the surface model to an NC machine to manufacture the physical shoelast model.

More systematic information on the relation between the foot and the shoelast is needed to make a shoelast that fits an individual foot. With the conventional shoelast design process, we cannot accumulate the shoelast data and the foot data in a database, not to mention extracting the relation between them. However, the proposed shoelast design system will provide a mechanism

for accumulating a large database of shoelast and foot data, from which better shoelast design rules can be derived.

In future work, it is necessary to make our algorithm compatible with current NURBS based CAD systems. In addition, the continuity between adjacent developable patches needs to be investigated in a systematic way.

Acknowledgments

The authors wish to acknowledge the financial support of the Korea Research Foundation made in the program year (1999).

References

Cho, M., 1985, "Research Report on Standardization of Foot Measuring Body and Shoelast Design," *KAIST*

Craig, J., 1986, "Introduction to Robotics Mechanics & Control," *Addison-Wesely Publishing Co.*, pp. 42~46.

do Carmo, M. P., 1976, Differential Geometry of Curves and Surfaces., *New Jersey: Prentice-Hall*, Englewood Cliffs.

Elber, G. 1995. Model Fabrication Using Surface Layout Projection. *Comput.-Aided Des.*, Vol. 27, No. 4, pp. 283~291.

Miller, R. G., 1976, *Manual of Shoemaking*, C. & J. Clark Ltd. Printing Department

Park, F. C., Yoo, J., and Ravani, B., 1999. Optimal Control and the Design of Developable Surfaces. *Comput.-Aided Des. under review.*

Piegl, L. and Tiller, W., 1995, *The NURBS Book*, Springer-Verlag, pp. 410~413

Tsai, R. Y., 1986, "A Versatile Camera Calibration Technique for High Accuracy 3d Machine Vision Metrology Using Off-the-Shelf TV Cameras and Lenses," *IEEE J. Robotics Automat.*, Vol. 3, pp. 323~344.